Available online at www.sciencedirect.com

SciVerse ScienceDirect

Physics Procedia 36 (2012) 1248 – 1253

Physics Procedia

Superconductivity Centennial Conference

Modelling and simulation of inductive fault current limiters

João Murta Pina[a*], Pedro Pereira[a], Anabela Pronto[a], Pedro Arsénio[b], Tiago Silva[b]

[a]*Centre of Technology and Systems, Faculdade de Ciências e Tecnologia, Monte de Caparica, 2829-516 Caparica, Portugal*
[b]*Dep. Electrical Engineering, Faculdade de Ciências e Tecnologia, Monte de Caparica, 2829-516 Caparica, Portugal*

Abstract

Inductive superconducting fault current limiters have already demonstrated their technical viability in electrical networks. Its architecture and robustness make them potentially adequate for distribution networks, and this type of devices is considered as an enabling technology for the advent of embedded generation with renewable energy sources. In order to promote the growth and maturity of these superconducting technologies, fast design tools must be developed, allowing simulating devices with different materials in grids with diverse characteristics. This work presents advances in the development of such tool, which, at present stage, is an effective alternative to software simulations by finite elements methods, reducing dramatically computation time. The algorithms are now compared with experimental results from a laboratory scale prototype, showing the need to refine them.

Keyword: Superconducting Fault Current Limiters; Inductive Limiters; Magnetic Shielding Limiters

1. Introduction

Inductive superconducting fault current limiters (FCL) have been originally proposed in 1991 [1] and its technical viability has already been demonstrated [2]. They can be built by a high temperature superconducting (HTS) cylinder magnetically linked with the power line (primary), and its operation has been far described elsewhere, see e.g. [3]. Simplicity of construction and robustness make them attractive in particular applications, as microgrids [4] or networks with dispersed generation [5]. The simulation of inductive FCLs is often performed by finite elements method (FEM) software, as Flux2D, from Cedrat Company. However, simulations can last for hours or days, only for small scale devices in simple grids. Simulation of real size limiters, in realistic complex grids, is thus not feasible with FEM. The purpose of

* Corresponding author.
E-mail address: jmmp@fct.unl.pt.

1875-3892 doi:10.1016/j.phpro.2012.06.284

this work is to develop methods that can be used to perform fast dynamic simulations of inductive limiters. A first goal is to base those developments on Flux2D simulations, which is used e.g. in [6]. After that, results are compared with experiments, showing important differences. The approach used starts by original modelling of these devices. Inductive FCLs are often modelled by transformer-like equivalent schemes, see e.g. [2]. However, these do not account for iron non-linearity, which determines the behaviour of the FCL. In other cases, devices are modelled by time-dependent impedances; see e.g. [7]. Although HTS impedance changes with time, it is due to current, flux density and temperature dependences, not on time. The proposed model, whose basis was already described by the authors [8], surpasses these restrictions.

2. FCL simulation methodology based on finite elements simulations

2.1. Topology of the limiter

The developed methodology uses results from a small scale model with bulk HTS cylinder as a secondary. Fig. 1.(a) shows simulation results of the linked flux of a closed core FCL, ψ (core dimensions shown in Fig. 1.(b)), as a function of the line current, i, considering different values of short-circuit current, I_{SC}. Excursions in the $i-\psi$ plane lie roughly on the same maximum hysteresis loop. Thus, the behaviour of the limiter depends on this loop, and this is the basis of the proposed methodology, which defines how to build it from data of the parts of the limiter (core and cylinder), and grid characteristics (short-circuit current). After that, the dynamic behaviour of devices is simulated in a much faster way than using FEM software. Table 1 describes the characteristics of the cylinder and primary.

2.2. Comparison of the hysteresis loops of the limiter and its iron core

The iron core determines the behaviour of the limiter, as shown in the sequel. The electromagnetic characteristics of the primary with core inserted, but without HTS cylinder, ψ_0, is plotted in Fig. 2.(a), as well as the excursion in the $i-\psi$ plane, ψ_{FCL}. The core is built by electrical steel from Flux2D library, reference FLU_M27035A. It is clear that ψ_{FCL} follows a path parallel to ψ_0. The behaviour of the limiter is exemplified in Fig. 2.(b), for a grid under a fault applied at $t = 20\,\text{ms}$. Limitation is achieved in the vertical branches of the hysteresis loop. In saturation this is nearly horizontal, and current is only limited by grid impedance.

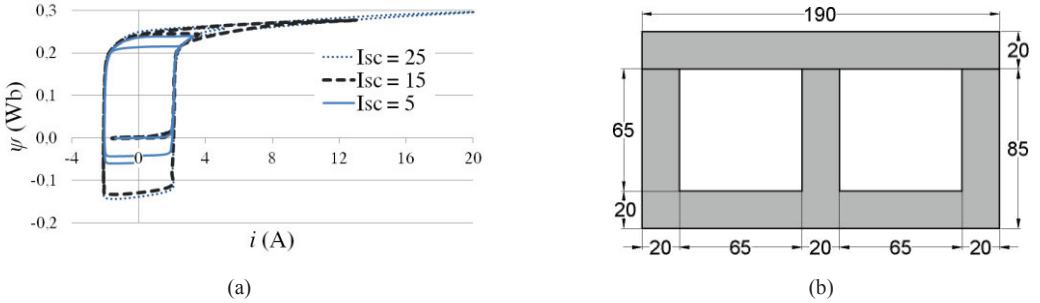

(a) (b)

Fig. 1. (a) Simulation results obtained using Flux2D, showing for a particular inductive limiter the excursion of the linked flux, ψ, of its primary as a function of the line current, i, under a fault. The observed excursions lie approximately on the same maximum hysteresis loop; (b) Dimensions of the magnetic core of the limiter, where thickness is 20 mm, and all dimensions are in millimetres.

Table 1. Parameters of the HTS cylinder and primary of the limiter

HTS cylinder (Bi-2223)	Value	Primary	Value
Internal radius (mm)	16.5	Number of turns	350
Width (mm)	2.5	Radius (mm)	23.0
Height (mm)	48.0	Height (mm)	35.0
Critical current @ 77 K (A)	360		
n value	15		

2.3. Assembly of the maximum hysteresis loop of the FCL

The maximum hysteresis loop is built by parameters from the constitutive parts of the limiter, namely the maximum induced current of the HTS cylinder and the electromagnetic characteristic of the iron core.

The maximum induced current in the HTS cylinder under external applied field is defined as I^*_{HTS}. In Flux2D, the primary was fed with a sinusoidal current (42 kA·turn amplitude) and current through cross section of the cylinder was calculated, see Fig. 3, where $I^*_{HTS} = 694$ A, almost twice the critical current.

The characteristic of the core, defined as the relation between the current in the primary, i, and the linked flux, ψ_0, without HTS cylinder, is modelled analytically by

$$\psi_0(i) = aNi + \frac{bNi}{c + dN|i|} \tag{1}$$

where a, b, c and d are fitting parameters and N is the number of primary turns. The characteristic must be obtained at cryogenic operating temperature, as it may differ from the one obtained at room temperature [9]. Fitted parameters are $a = 7.34\times10^{-6}$, $b = 6.23$, $c = 457.8$ and $d = 25.2$. The FCL's maximum hysteresis loop, ψ^*_{FCL}, is built with the previous data. The descending and ascending loop branches cross current's axis at $\pm I^*_{HTS}/N$, since these are the maximum currents whose flux densities the HTS can shield.

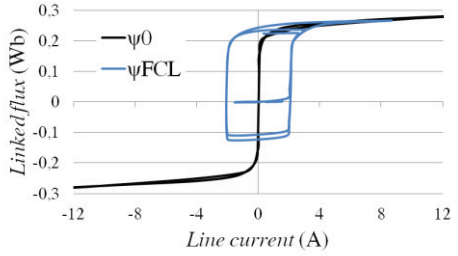

(a)

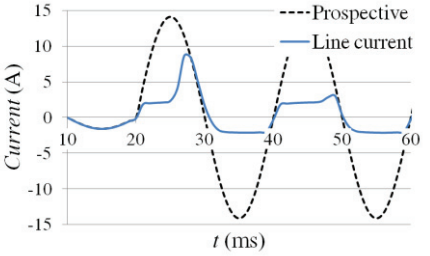

(b)

Fig. 2. (a) Comparison of the excursion in the $i-\psi$ plane of the limiter under a fault, ψ_{FCL}, and electromagnetic characteristic of the primary with core inserted and without HTS cylinder, ψ_0. In ψ_{FCL} the region corresponding to approximately zero linked flux corresponds to normal operation, while the hysteresis loop corresponds to behaviour under a fault; (b) Time evolution of the current after a short-circuit applied at $t = 20$ ms. The 10 A_{rms} prospective current is also shown.

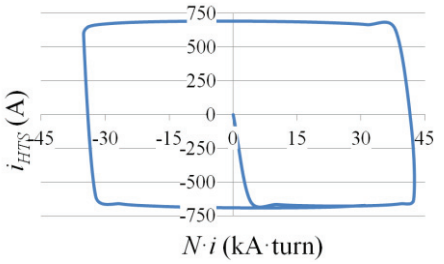

Fig. 3. Determination of the maximum induced current in the HTS cylinder. The current in the cylinder, i_{HTS}, is generated by reaction to the flux density due to the current in the primary winding, i. Maximum current establishes at 694 A amplitude.

The branches are determined using an auxiliary function, $f(i)$, and the characteristic ψ_0, as represented in Fig. 4.(a), according to $\lambda_a(i) = \psi_0(i - f(i))$ and $\lambda_d(i) = \psi_0(i + f(i))$, where λ_a and λ_d are, respectively, the ascending and descending branches of the maximum hysteresis loop. The auxiliary function $f(i)$ is defined in [8]. The ascending and descending branches merge in ψ_0, should current fall outside $\pm I_{SC}$, although this value has little influence on the shape of the loop, under certain limits.

2.4. Methodology for the dynamic simulation of inductive FCL

The maximum loop is used to simulate the dynamic behaviour of the grid under a fault. In order to clearly illustrate this, a single phase grid built by a voltage source, u, and lumped parameters that model grid's short-circuit impedance, namely resistance R, inductance L, and capacitance C, is considered. The Euler-Cauchy [10] method is applied to solve circuit equations, and the excursion in the $i-\psi$ plane is determined according to the simple algorithm proposed in [8].

2.5. Evaluation of the dynamic behaviour of the limiter

One result of the methodology is presented in Fig. 5, for a single-phase grid with short-circuit impedance $R = 5\,\Omega$, $I_{SC} = 10\,\mathrm{A_{rms}}$, and two consecutive faults of 19 ms each, applied at $t = 20$ and $t = 74$ ms. Comparison with FEM simulations is also presented, showing a clear agreement.

3. Comparison of the proposed methodology with experimental results

Although the developed methodology may replace FEM long time simulations, it must be compared with experimental results, in order to be fully validated. A laboratory scale model was built according to previous dimensions. The HTS cylinder was acquired to CAN Superconductors, model CST-33/48.1.

3.1. Determination of the characteristics of the constitutive parts of the limiter

The first part of the methodology consists on evaluating the maximum induced current in the cylinder and determining the electromagnetic characteristic of the core. This is done supplying the primary with only the HTS cylinder inserted with sinusoidal currents of different amplitudes, and measuring the current in the cylinder with a Rogowski coil. Results are plotted in Fig. 6.(a), and they differ from Fig. 3. The measured characteristic of core is represented in Fig. 6.(b).

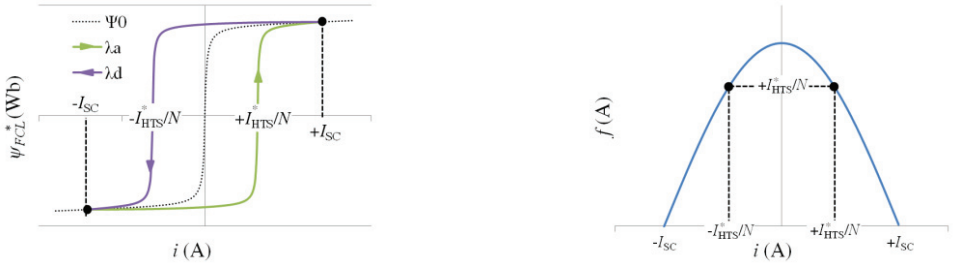

Fig. 4. (a) General maximum hysteresis loop, ψ^*_{FCL} , of an inductive FCL; (b) Auxiliary function f used to build the ascending and descending branches of the loop, λ_a and λ_d respectively.

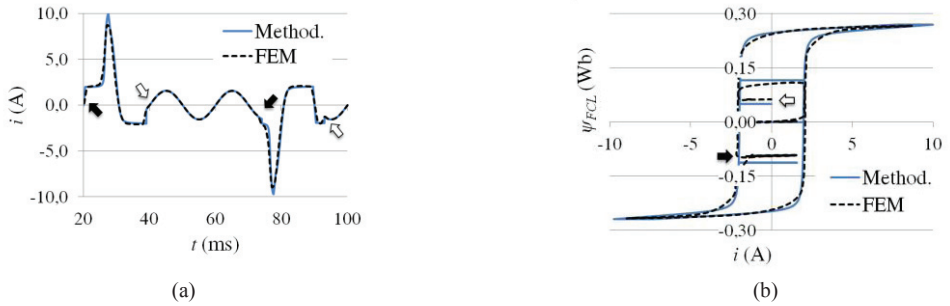

Fig. 5. Comparison of results with proposed methodology and FEM, in a resistive grid and two consecutive 19 ms faults ($t = 20$ ms and $t = 74$ ms). (a) Evolution of current, black arrows point to fault initiation and white arrows to faults clearance; (b) Excursion in $i - \psi$ plane, black and white arrows point to the FCL magnetic states after first and second faults are cleared, respectively.

3.2. Evaluation of the dynamic behaviour of the limiter

Different tests were performed on the limiter. In Fig. 6.(c), the excursion in the $i - \psi$ plane is plotted, for 50 V_{rms} supply voltage and 0.72 Ω short-circuit resistance. Unlike the observed in FEM simulations, see Fig. 2.(a), the excursion is not parallel to the characteristic of the core, rather appears rotated.

4. Discussion

From experimental results, it is clear that the proposed methodology must be adapted in order to comprise a valid simulation tool. In fact, the rotation observed in ψ_{FCL} relatively to ψ_0 is due to the different behavior of the induced current in the HTS cylinder, which has to be included in the models.

5. Conclusions and future work

A methodology for the simulation of inductive FCL was presented in this paper. One potential application is the design of these devices, testing different materials, number of turns, or even grid parameters. The motivation for this work was avoiding the long computation times needed with Flux2D, several hours or days, reduced to nearly one second with the proposed methodology running in Matlab. In order to correctly apply this methodology to real devices, measurements were performed on a small scale

prototype, demonstrating the need to adjust the models. This is currently being performed, aiming to model the induced current in the HTS cylinder as a function of the magnetomotive force of the primary. Future work includes replacing the cylinder by 2G tape and the inclusion of temperature in the models.

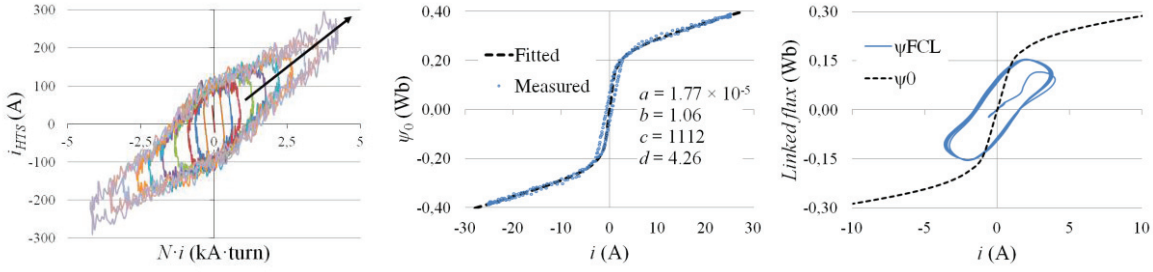

Fig. 6. Experimental results obtained with the prototype. (a) Induced current in the HTS cylinder as a function of growing magnetomotive force in the primary, without iron core; (b) Measured and fitted characteristics of the primary with iron core and without HTS. (c) Excursion in the $i-\psi$ plane under a fault, ψ_{FCL}, and electromagnetic characteristic of the primary ψ_0.

Acknowledgements

This work is funded by National Funds through FCT – Fundação para a Ciência e a Tecnologia, under project PEst-OE/EEI/UI0066/2011.

References

[1] Bashkirov Y, Fleishman L, Patsayeva T, Sobolev A, Vdovin A. Current-limiting reactor based on high-T_C superconductors. *IEEE Trans. Mag.* 1991; **27**: 1089-92.

[2] Paul W, Lakner M, Rhyner J, Unternährer P, Baumann Th, Chen M, Widenhorn L, Guérig A. Test of 1.2 MVA high-T_C superconducting fault current limiter. *Supercond. Sci. Technol.* 1997; **10**: 914-8.

[3] Noe M, Steurer M. High-temperature superconductor fault current limiters: concepts, applications and development status. *Supercond. Sci. Technol.* 2007; **20**: R15-29.

[4] Jiayi H, Chuanwen J, Rong X. A review on distributed energy resources and MicroGrid. *Renew. Sust. Energy Rev.* 2008; **12**: 2472-83.

[5] Pina J M, Ventim Neves M, Alvarez A, Rodrigues A L. High temperature superconducting fault current limiters as enabling technology in electrical grids with increased distributed generation penetration. In: Camarinha-Matos L, Pereira P, Ribeiro L, editors. *Emerging Trends in Technological Innovation*, Springer Boston; 2010, 427-34.

[6] Kozak S, Janowski T, Wojtasiewicz G, Kozak J, Glowacki B A. Experimental and numerical analysis of electrothermal and mechanical phenomena in HTS tube of inductive SFCL. *IEEE Trans. Appl. Supercond.* 2006; **16**: 711-4.

[7] Yamaguchi H, Kataoka T. Current limiting characteristics of transformer type superconducting fault current limiter with shunt impedance and inductive load. *IEEE Trans. Appl. Supercond.* 2008; **18**: 668-71.

[8] Pina J M, Suárez P, Ventim Neves M, Rodrigues A L. Reverse engineering of inductive fault current limiters. *J. Phys.: Conf. Ser.* 2010; **234**: 032047.

[9] Pronto A G, Ventim Neves M, Rodrigues A L. Measurement and separation of magnetic losses at room and cryogenic temperature for three types of steels used in HTS transformers. *J. Supercond. Novel Magnet.* 2011; **24**: 981-5.

[10] Bird J. *Higher Engineering Mathematics*. 5th ed. Newnes; 2007.